Molecular Therapy
Nucleic Acids
Original Article

The Circular RNome of Developmental Retina in Mice

Xue-Jiao Chen,[1,2,4] Zi-Cheng Zhang,[3,4] Xiao-Yun Wang,[1,2,4] Heng-Qiang Zhao,[3] Meng-Lan Li,[1,2] Yue Ma,[1,2] Yang-Yang Ji,[1,2] Chang-Jun Zhang,[1,2] Kun-Chao Wu,[1,2] Lue Xiang,[1,2] Lan-Fang Sun,[1,2] Meng Zhou,[2,3] and Zi-Bing Jin[1,2]

[1]Laboratory for Stem Cell and Retinal Regeneration, Institute of Stem Cell Research, Division of Ophthalmic Genetics, The Eye Hospital, Wenzhou Medical University, Wenzhou 325027, China; [2]State Key Laboratory of Ophthalmology, Optometry and Vision Science, Wenzhou Medical University, National Center for International Research in Regenerative Medicine and Neurogenetics, Wenzhou 325027, China; [3]School of Ophthalmology & Optometry and Eye Hospital, School of Biomedical Engineering, Wenzhou Medical University, Wenzhou 325027, China

Circular RNAs (circRNAs) represent a class of noncoding RNAs with a wide expression pattern, and they constitute an important layer of the genome regulatory network. To date, the expression pattern and regulatory potency of circRNAs in the retina, a key part of the central nervous system, are not yet well understood. In this study, RNAs from five stages (E18.5, P1, P7, P14, and P30) of mouse retinal development were sequenced. A total of 9,029 circRNAs were identified. Most circRNAs were expressed in different stages with a specific signature, and their expression patterns were different from those of their host linear transcripts. Some circRNAs could act as sponges for several retinal microRNAs (miRNAs). Furthermore, *circTulp4* could function as a competitive endogenous RNA (ceRNA) to regulate target genes. Remarkably, silencing *circTulp4 in vivo* led to mice having a thin outer nuclear layer (ONL) and defective retinal function. In addition, we found that circRNAs were dysregulated at a much earlier time point than that of disease onset in a retinal degeneration model (rd8 mice). In summary, we provide the first circRNA expression atlas during retinal development and highlight a key biological role for circRNAs in retinal development and degeneration.

INTRODUCTION

circRNAs (circular RNAs) are a novel class of noncoding RNAs with tissue- and stage-specific expression patterns, and they are much more stable than linear transcripts.[1,2] To date, a large number of circRNAs have been identified and characterized in various cell lines and across different species.[3–5] In addition, the expression patterns and biological functions of circRNAs in the vertebrate brain have been widely studied.[1,6–10] circRNAs are highly abundant in the brain, with specific and dynamic expression patterns during neuronal differentiation.[1] Notably, circRNAs may regulate synaptic activity and brain function during development; for example, *Cdr1as*, which is one component of a regulatory RNA network in the brain, is essential for normal brain function.[11,12] These findings show that circRNAs are highly expressed in the central nervous system (CNS) in a spatio-temporal-dependent manner.

Recently, circRNAs were reported to participate in a wide range of biological processes and to be differentially expressed in various diseases, including cancer,[13–15] neurological disorders,[16,17] and diabetic retinopathy.[18,19] The abundant expression, conservation, specificity, and stability of circRNAs allow them to play potential roles as biomarkers for diagnosis, prognosis, and as predictors of the therapeutic response to treatments.[14,19–21] However, the molecular mechanisms involved in the biological processes of circRNAs and the functions of those circRNAs *in vivo* remain largely unknown.

As a key but separate part of the CNS, the retina is an essential component of the eye and is responsible for vision production by transducing light signals into neuronal signals. Currently, if and how circRNAs are involved in retinal development and degeneration remains largely unknown. Profiling retinal circRNAs from different stages of development and degeneration would not only help us understand their physiological function, but also provide a circRNA-based therapeutic strategy for retinal diseases. In this study, we attempted to investigate the circRNA expression profile during retinal development and found that circRNAs were abundantly expressed during this process. Several circRNAs were found to serve as microRNA (miRNA) sponges. Strikingly, *circTulp4* was validated to be essential for retinal function *in vivo*. Furthermore, the expression of circRNAs seemed more variable than that of linear transcripts in a retinal degeneration model, implying that circRNAs could act as biomarkers for retinal diseases. Our findings indicate that circRNAs

Received 9 May 2019; accepted 9 November 2019;
https://doi.org/10.1016/j.omtn.2019.11.016.

[4]These authors contributed equally to this work.

Correspondence: Zi-Bing Jin, Laboratory for Stem Cell and Retinal Regeneration, Institute of Stem Cell Research, Division of Ophthalmic Genetics, The Eye Hospital, Wenzhou Medical University, Wenzhou 325027, China.
E-mail: jinzb@mail.eye.ac.cn
Correspondence: Meng Zhou, State Key Laboratory of Ophthalmology, Optometry and Vision Science, Wenzhou Medical University, National Center for International Research in Regenerative Medicine and Neurogenetics, Wenzhou 325027, China.
E-mail: zhoumeng@wmu.edu.cn

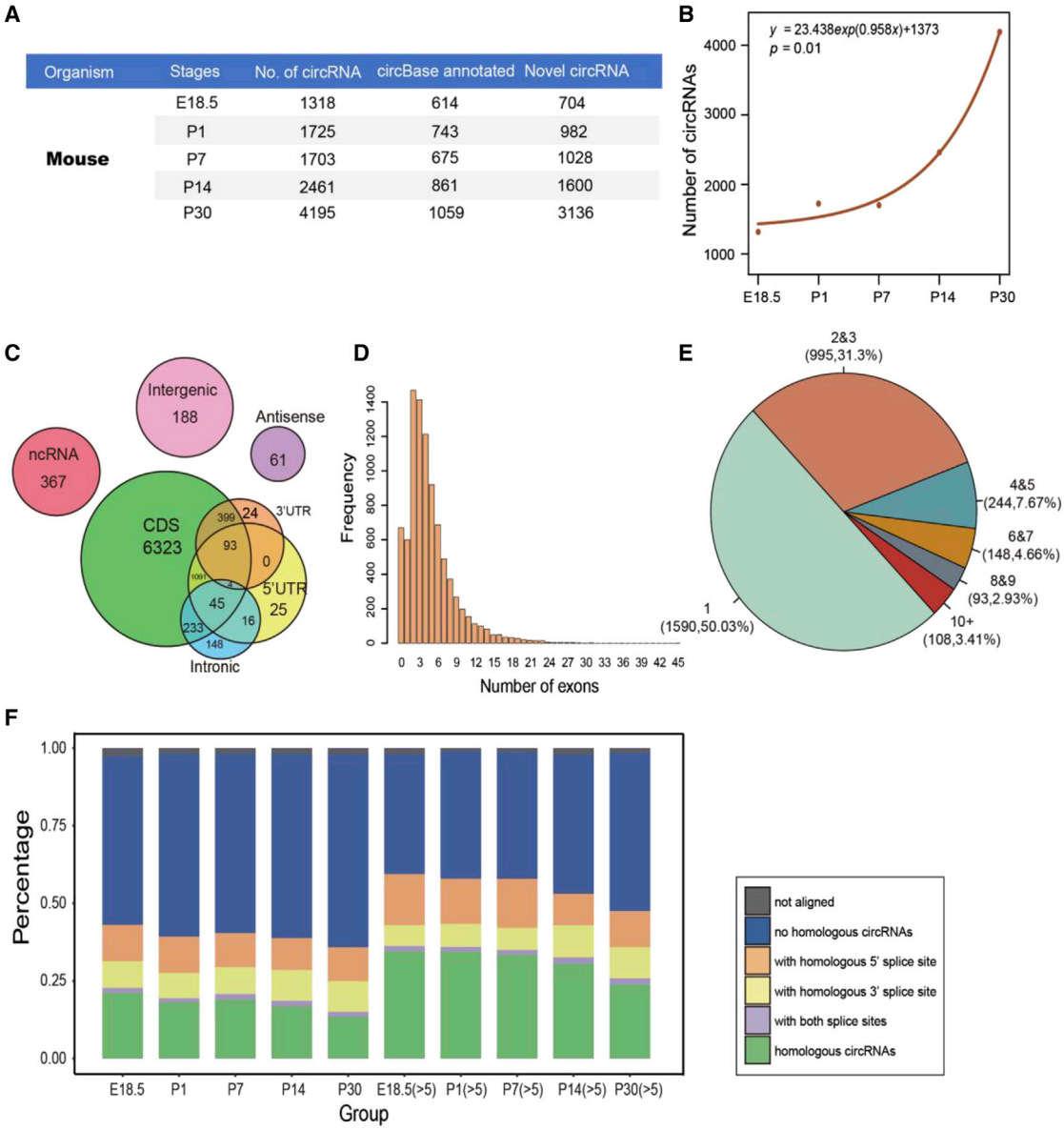

Figure 1. Identification and Characterization of circRNAs in the Mouse Retina

(A) Summary of circRNAs detected in the mouse retina during five developmental stages. (B) The number of circRNAs across the five developmental stages. (C) Genomic origins of mouse circRNAs. (D) Numbers of circRNAs produced from one gene. (E) Exon number distributions for the mouse circRNAs. (F) Conservation analysis for circRNAs in the retina compared between humans and mice (x axis represents circRNAs in the five stages mouse retinas, all circRNAs [left] and circRNAs ≥5 reads [right]).

possess distinct signatures and play essential roles in retinal developmental stages and function.

RESULTS

Identification and Characterization of circRNAs in the Mouse Retina

To comprehensively reveal the stage-specific expression patterns of circRNAs in the mouse retina on a genomic scale, we performed transcriptome profiling of circRNAs by deep RNA sequencing (RNA-seq) of ribosomal RNA-depleted total RNA samples. The samples came from five developmental stages, including the embryonic stage (E18.5), early postnatal stage (P1), outer segment of photoreceptor development stage (P7),[22] eye opening stage (P14), and maturation (P30). A total of 9,029 unique circRNAs present during retinal development were detected using the find_circ and CIRI computational pipelines (Figure 1A). We found that most circRNAs (5,616, 62.20%) were novel and that only 3413 circRNAs (37.80%) had been annotated in circBase to date.[3] Furthermore, the number of

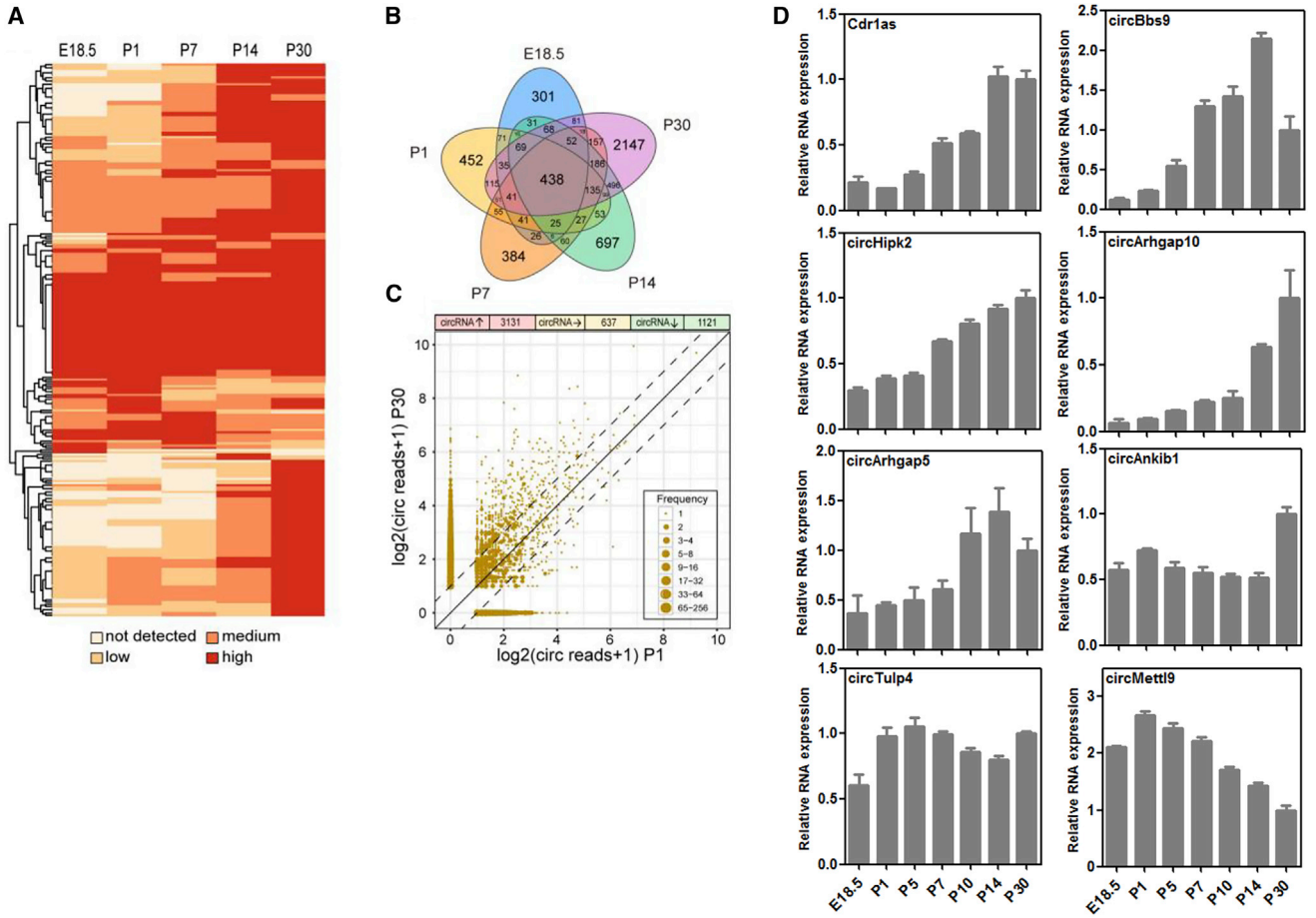

Figure 2. Expression Pattern of circRNAs during Retinal Development

(A) Heatmap comparisons of circRNAs during the five developmental stages. (B) Venn diagram showing the expression patterns of circRNAs across the five stages. (C) circRNAs with $\log_2$-fold changes between P30 and P1; the dashed line represents the 2-fold cutoff. (D) qRT-PCR validation of circRNA expression during retinal maturation (n = 5, the normalized values represent the mean ± SEM).

circRNAs increased rapidly during retinal development (Figures 1A and 1B). A total of 4,195 circRNAs were detected at P30, accounting for 46.46% of the total circRNAs in the retina.

We also examined the distribution of the genomic origins of total circRNAs and found that most circRNAs (8,188, 90.69%) originated from coding sequence (CDS) exons, whereas only a small fraction was derived from UTR, intergenic, non-coding RNA (ncRNA), and antisense sequences (Figure 1C). Typically, circRNAs from CDS exons were encoded by three to six exons (Figure 1D). Most of the 3,030 host genes (1,590, 52.48%) produced only one circRNA, while a few genes (108, 3.56%) produced more than 10 circRNAs (Figure 1E). Next, we analyzed circRNA conservation between humans[23] and mice using the method previously reported by Rajewsky et al.[1,24] More than 13.48% of the circRNAs identified at each developmental stage were expressed in the human retina (Figure 1F). Furthermore, highly expressed mouse circRNAs (>5 reads) were more likely to be conserved in humans at each time point. These results collectively revealed the abundant expression and the spatiotemporal pattern of circRNAs in the retina.

Expression Patterns of circRNAs during Retinal Development

To obtain an overview of the circRNA expression pattern during retinal development, we further profiled the circRNAs at five time points (Data S3). We found that circRNAs were enriched and upregulated during retinal development (Figure 2A). Most circRNAs were specifically expressed at different stages and had a specific signature (Table S1); however, 438 circRNAs were expressed at all tested stages (Figure 2B). Many circRNAs were upregulated during retinal development, especially at P14 and P30 (Figure 2C; Figure S1; Data S4).

Next, circRNAs with dynamic or high expression patterns during retinal development or those derived from host genes with important roles in the retina were selected for further experimental

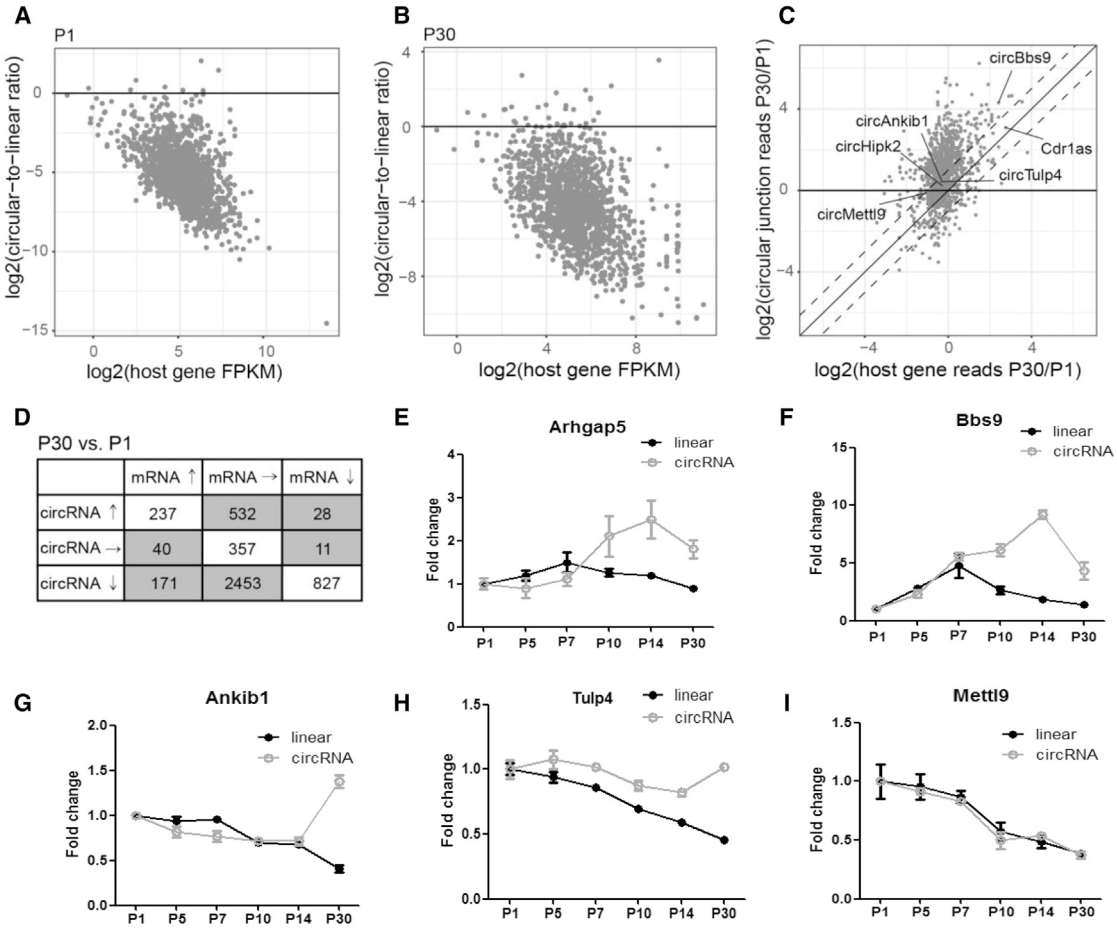

Figure 3. circRNA and Linear mRNA Expression Changes Differ during Retinal Development

(A–D) Quantification of circRNAs and mRNAs during retinal development. (A and B) Circular-to-linear ratio plotted against the host gene TPM at P1 (A) and P30 (B). (C) circRNA expression changes between the P1 and P30 stages of development are positively correlated with expression changes of the host genes. (D) Summary of circRNA and host gene expression changes. (E–I) qRT-PCR validation of circRNA and host gene expression during retinal development (n = 5, the normalized values represent the mean ± SEM). (E) *Arhgap5*, (F) *Bbs9*, (G) *Ankib1*, (H) *Tulp4*, and (I) *Mettl9*.

validation. Seven of the eight selected circRNAs were derived from a protein coding region (CDS), including *circBbs9*, *circHipk2*, *circArhgap10*, *circArhgap5*, *circAnkib1*, *circTulp4*, and *circMettl9*. The predicted head-to-tail junction sequences of these circRNAs were confirmed by Sanger sequencing (Figure S2). Additionally, the expression patterns of the circRNAs were validated by quantitative RT-PCR (qRT-PCR) (Table S2). Among the eight selected circRNAs, five (*Cdr1as*, *circBbs9*, *circHipk2*, *circArhgap10*, and *circArhgap5*) were upregulated during retinal development, one (*circMettl9*) was downregulated, and two (*circAnkib1* and *circTulp4*) remained unchanged (Figure 2D). Note that the expression patterns of these circRNAs as determined by the qRT-PCR results were not fully consistent with the RNA-seq results (Figure S3), indicating a flaw in the circRNA detection algorithm, which has been described in a previous study.[25] In brief, we demonstrated for the first time the expression patterns of retinal circRNAs during development.

circRNA and Linear Transcript Changes Differ during Retinal Development

Previous studies have reported that most circRNAs and linear transcripts from the same host gene have distinct expression patterns during development and between cell types.[5,26] We combined the circular-to-linear ratio (CLR) with host gene mRNA expression (fragments per kilobase of transcript per million mapped reads [FPKM]),[1] and a negative correlation was found between host gene expression and the CLR at P1 and P30 (Figures 3A and 3B), which is inconsistent with the view that circRNAs are a byproduct of occasional aberrant splicing.[27,28] In addition, the expression of most circRNAs was lower than that of the corresponding host gene ($\log_2$ CLR < 0; most genes were below the black solid line), and highly expressed host genes produced fewer circRNAs (higher FPKM and lower CLR). The changes in circRNAs and their host genes during retinal development were correlated (Figures 3C and 3D; Figures S4A–S4D), and more circRNAs tended to be upregulated (ordinate

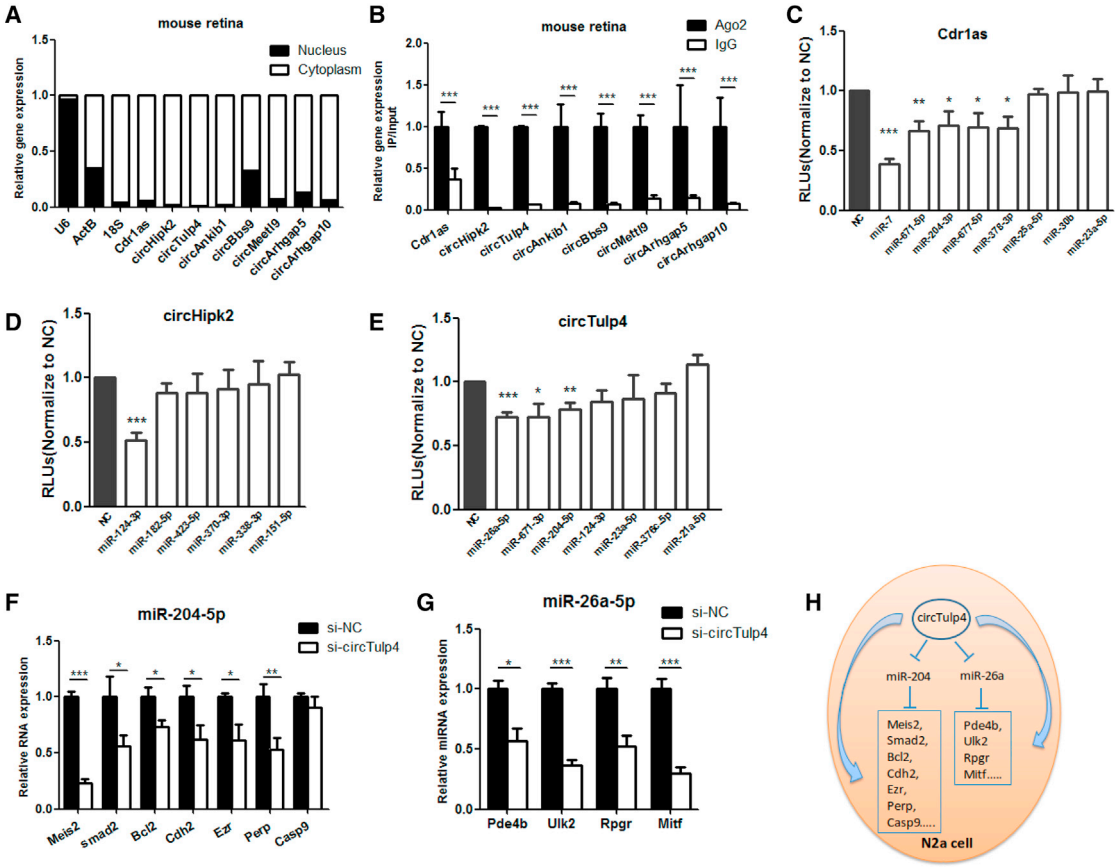

Figure 4. circRNAs Function as ceRNAs to Regulate Target Genes

(A) qRT-PCR detection of circRNAs in the nuclear and cytoplasmic fractions isolated from mouse retinas. U6 is a nuclear transcript used as a control, and ActB and 18S are cytoplasmic transcripts used as controls (n = 3). (B) qRT-PCR detection of immunoprecipitated circRNAs in the mouse retina using Ago2 and IgG antibodies (n = 3). (C–E) Luciferase assay detection of binding between miRNAs and *Cdr1as* (C), *circHipk2* (D), and *circTulp4* (E) in 293D cells (n = 3 per group). (F and G) qRT-PCR detection of the miR-204-5p (F) and miR-26a-5p (G) target genes in N2a cells after transfection with si-circTulp4 (n = 3). (H) A model summarizing the circTulp4-miR204/miR-26a-mRNA network in N2a cells. The normalized values represent the mean ± SEM. *$p < 0.05$, **$p < 0.005$, ***$p < 0.001$, Student's t test.

values greater than 0), indicating the important role of circRNAs in retinal development. Notably, circRNAs levels were more variable than host genes levels. For instance, the expression level of 2,985 circRNAs was changed, while the corresponding host genes were unaltered (P30 versus P1); the expression of 51 host genes was changed, while the corresponding circRNA remained unchanged (Figure 3D). A similar pattern was found at P7 versus P1 and P14 versus P1 (Figure S4).

Next, we validated the expression patterns of selected circRNAs and their host linear transcripts by using qRT-PCR. *circArhgap5*, *circBbs9*, and *circAnkib1* increased, whereas their linear transcripts decreased during retinal development (Figures 3E–3G). In contrast, *circTulp4* had a high expression pattern that remained unchanged during development, whereas the host mRNA continually decreased (Figure 3H). In addition, *circMettl9* expression had the same expression tendency between the circRNA and mRNA during retinal development (Figure 3I). Taken together, bioinformatics analysis and quantitative assays indicated that the expression levels of circRNAs and their corresponding linear transcripts differed throughout retinal development.

circTulp4 Functions as a Competitive Endogenous RNA to Regulate Target Genes

To initially explore the function of the circRNAs identified in the mouse retina, the eight selected circRNAs were studied in a functional investigation. The nuclear versus cytoplasmic enrichment assay showed that the tested circRNAs were predominantly expressed in the cytoplasm (Figure 4A). Because miRNAs exist in the cytoplasm and Ago2 is the core component of the RNA-induced silencing complex (RISC) that binds miRNAs to target mRNAs,[29] we attempted to determine whether circRNAs could interact with miRNAs by performing RNA immunoprecipitation (RIP) using an antibody against Ago2. The results showed that all of the studied circRNAs were enriched in the Ago2 protein fraction (Figure 4B), implying that these circRNAs could interact with miRNAs.

To further confirm the binding of circRNAs and miRNAs, bioinformatics analysis based on miRanda, RNAhybrid, and TargetScan was performed. We revealed that retina-associated miRNAs could bind the circRNAs studied here (Data S2). Subsequently, Luci-circRNAs were constructed to verify binding between circRNAs and miRNAs. *Cdr1as* was reported to act as a miR-7 and miR-671-5p sponge, so we performed a luciferase assay for other miRNAs. We found that *Cdr1as* acting as sponge of miR-204-3p, miR-677-5p, and miR-378-3p (Figure 4C), *circHipk2* acting as sponge of miR-124-3p (Figure 4D), and *circTulp4* acting as sponge of miR-26a-5p, miR-671-3p, and miR-204-5p (Figure 4E). Other results from the luciferase assay that were performed to detect the sponge activity of circRNAs and miRNAs were summarized in Figure S5. The target sites of miRNAs on corresponding circRNAs were shown in Figure S6. These results demonstrated the potential roles of these circRNAs as competitive endogenous RNAs (ceRNAs) to regulate retinal development.

Next, we studied whether *circTulp4* acted as a ceRNA by sponging miR-204-5p and miR-26a-5p. Small interfering RNAs (siRNAs) targeting the backsplice sequence of *circTulp4* were designed (Table S3). Transfection of si-circTulp4 into Neuro2a (N2a) cells demonstrated that si-circTulp4 significantly downregulated *circTulp4* expression but did not affect expression of the linear *Tulp4* transcripts (Figure S7).

Considering that circTulp4 could act as a miR-204-5p and miR-26a-5p sponge, miR-204-5p and miR-26a-5p activity could increase after si-circTulp4 transfection, leading to downregulation of the target genes of miR-204-5p (*Mesi2*, *Bcl2*, *Cdh2*, *Ezr*, *Perp*, and *Casp9*) and miR-26a-5p (*Pde4b*, *Ulk2*, and *Rpgr*). As expected, these genes were decreased significantly after si-circTulp4 transfection *in vitro* (Figure 4F). Collectively, these results suggested that retinal circRNAs could act as miRNA sponges, and *circTulp4* functioned as a ceRNA by acting as sponge for miR-204-5p and miR-26a-5p to regulate their corresponding target genes (Figures 4G and 4H).

circTulp4 Is Essential for Retinal Function in Mice

To further determine the function of *circTulp4* in the mouse retina, we introduced a GFP-carrying adeno-associated virus (AAV)-circTulp4 short hairpin RNA (shRNA) vector or a control into the subretinal space of mice at P30 (Figures 5A and 5B). Fundus images showed GFP-labeled AAV expressed at P60 (Figure 5C), indicating a successful injection of AAV. As a result, *circTulp4* expression decreased to 62.99% in the AAV-shRNA-circTulp4-treated retinas, while linear *Tulp4* expression remained unchanged (Figure 5D). An *in situ* hybridization (ISH) assay displayed *circTulp4* localization and expression in the mouse retina. The expression of *circTulp4* decreased significantly in the inner segment (IS), outer plexiform layer (OPL), and inner plexiform layer (IPL) (Figure 5E). DAPI staining showed a thinned ONL throughout the retina, indicating that serious photoreceptor degeneration occurred due to the *circTulp4* deficiency (Figure 5F). Then, electroretinography (ERG) was performed to evaluate the photoreceptor function. Mouse eyes treated with AAV-circTulp4-shRNA displayed attenuated scotopic and photopic ERG responses. For the scotopic response, the a-wave amplitudes decreased to 9.17%, and the b-wave amplitudes decreased to 9.87% in the shRNA-treated mice (Figure 5G; Figure S8). In addition, several genes promoting apoptosis, such as *Perp*, were upregulated in the circTulp4 interrupted retina (Figure 5H), which was further confirmed by a terminal deoxynucleotidyltransferase-mediated dUTP nick end labeling (TUNEL) assay. The apoptotic cells that appeared in ONL were consistent with the thinned ONL phenotype (Figure 5I). However, silencing of *circTulp4* did not lead to an obvious change in miR-204-5p and miR-26a-5p expression, nor did it result in the downregulation of their target genes, such as *Smad2*, *Mitf*, and *Cdh2*, except for *Meis2* (Figures S9A and S9B). As a transcription factor, the target genes of *Meis2* were not changed, including *Pax6*, *Tbx5*, and *Bmp4* (Figure S9C). These results suggested that *circTulp4* has functions addition to acting as a miR-204 and miR-26a sponge. The complex microenvironment and compensatory *in vivo* mechanisms warranted further exploration. Overall, these observations confirmed that *circTulp4* is indispensable for proper retinal function.

circRNAs Dysregulated in Retinal Degeneration Mice Model

To determine whether circRNAs are dysregulated in a retinal degeneration model, rd8 mice with a crb1 mutation[30] were analyzed. Retinal degeneration in rd8 mice started at P90. We investigated whether circRNA changes could be observed before the onset of disease. qRT-PCR was conducted to detect circRNA expression in the retinas of rd8 mice at P30. Remarkably, most of the selected circRNAs were significantly upregulated (Figure 6A); however, their linear transcripts had only minor changes (Figure 6B). These results implied that circRNAs were more responsive than their corresponding linear transcripts to intrinsic retinal damage. Combined with the results shown in Figure 5, we concluded that proper circRNA expression is essential for retinal development and function and that circRNA dysregulation was detrimental to retinal development.

Our results described in preceding sections showed that *circHipk2* and *circTulp4* could act as sponges of miR-124-3p (Figure 4C) and miR-204-5p/miR-26a-5p, respectively (Figure 4E). Next, we examined the target genes of these miRNAs in the retinas of rd8 mice and found a significant increase in the expression levels of many target genes (Figure 6C), including *Meis2*, *Smad2*, *Ulk2*, *Slc6a6*, *Stat3*, and *Mitf*. These results further support the hypothesis that circRNAs can function as ceRNAs, and that upregulation of circRNAs can lead to an increase in some miRNA target genes due to the ability of circRNAs to act as sponges for miRNAs.

DISCUSSION

Previous studies have reported that circRNAs possess important regulatory functions,[31] especially in the CNS,[9,11] which is substantially enriched with circRNAs. However, circRNA expression and function in the retina, which is a key part of the CNS, have not been well profiled, especially at different developmental stages and disease conditions. To address this gap in knowledge, we sequenced

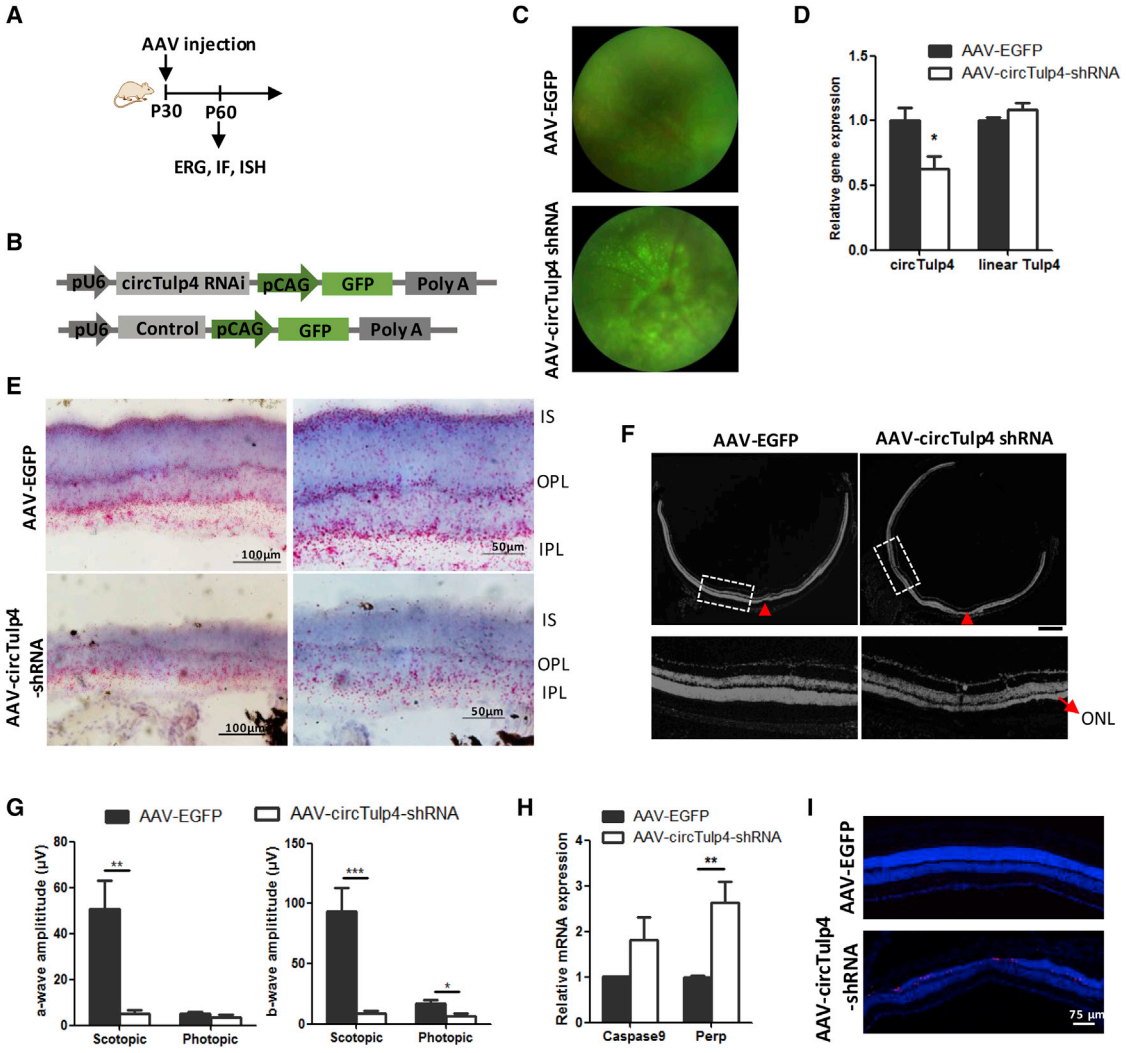

Figure 5. *circTulp4* Is Indispensable for Retinal Function in Mice

(A) Schematic representation of the experiment. (B) AAV-circTulp4 shRNA and AAV-EGFP expression cassettes driven by the pU6 promoter. (C) Fundus photographs of mice 1 month after AAV-circTulp4 shRNA or AAV-EGFP subretinal injection (n = 5). (D) Quantitative analysis of *circTulp4* and linear *Tulp4* in the retinas treated with AAV-circTulp4 shRNA and AAV-EGFP (n = 3). (E) Expression and localization of *circTulp4* after AAV-circTulp4 shRNA and AAV-EGFP subretinal injection; results are based on the BaseScope assay; red dots shows the sense of ISH image, and the negative control is shown in Figure S10 (n = 3). (F) The thickness of the nucleus in each retinal layer was assessed by DAPI staining (gray) after AAV-circTulp4 shRNA or AAV-EGFP subretinal injection (n = 3). The red arrowheads point to the AAV injection site, the red arrows point to the ONL, and the area in the white dotted box is enlarged at the bottom (n = 3) (G) The a-wave and b-wave amplitudes of the scotopic and photopic response after AAV-circTulp4 shRNA or AAV-EGFP subretinal injection (n = 5). (H) qRT-PCR detection of genes that promote apoptosis in the retina after AAV-circTulp4 shRNA or AAV-EGFP subretinal injection (n = 3). (I) Retinal cell apoptosis was assessed using a TUNEL assay, and TUNEL-positive cells (red) were observed in ONL. The normalized values represent the mean ± SEM. *p < 0.05, **p < 0.005, ***p < 0.001, Student's t test.

and analyzed circRNAs in the mouse retina (Data S4) and found that most circRNAs originated from exons; furthermore, circRNAs showed high expression and distinct signatures at different developmental stages (Figures 2A and 2B), which was consistent with data on circRNAs from the developmental rat retina,[2] indicating the important roles of circRNAs at certain retina stages. Additionally, circRNAs showed dynamic expression independent of their linear transcripts (Figure 3). circRNAs changed more dramatically than did their linear transcripts at each critical developmental time point (Figure 3D; Figure S4). Our findings indicated that circRNAs were involved in complex physiologic processes due to their specificity and variability.

By implementing bioinformatics tools and experimental verification, circRNAs acting as ceRNAs during retinal development were identified. Eight circRNAs (*Cdr1as*, *circBbs9*, *circHipk2*, *circArhgap10*, *circArhgap5*, *circAnkib1*, *circTulp4*, and *circMettl9*) with a dynamic and high expression pattern during retinal development were

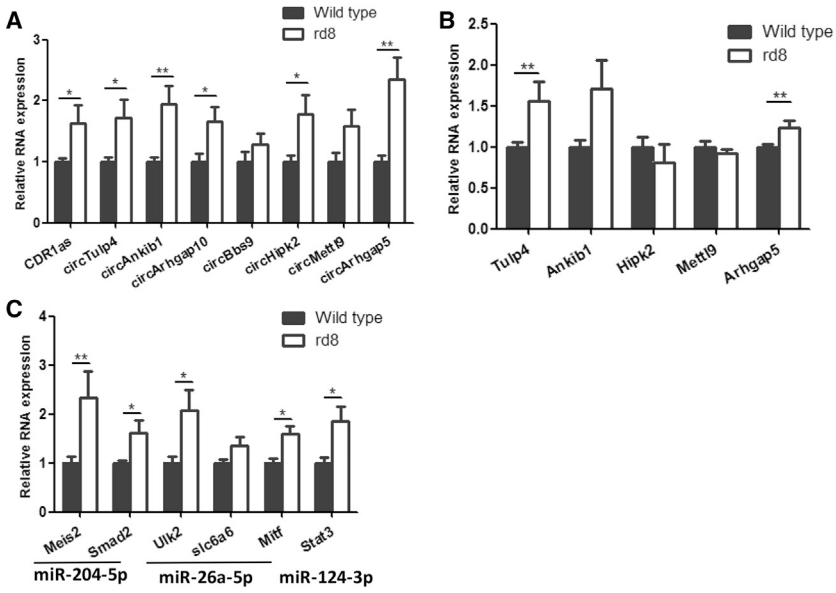

Figure 6. circRNAs Are Dysregulated in the rd8 Mouse Model

(A and B) qRT-PCR assay detection of circRNAs (A) and host linear mRNA (B) expression in the retinas of wild-type (WT) and rd8 mice. (C) qRT-PCR assay detection of miRNA target gene expression in the retinas of WT and rd8 mice. The normalized values represent the mean ± SEM. *$p < 0.05$, **$p < 0.005$, Student's t test. n = 5 per group.

selected for further experimental validation. However, only four circRNAs (*Cdr1as*, *circHipk2*, *circAnkib1*, and *circTulp4*) were confirmed to target miRNAs in the retina. For example, *Cdr1as* was miR-204/677/378 sponge, *circHipk2* was miR-124 sponge, *circTulp4* was miR-26a/671/204 sponge, and *circAnkib1* was miR-195a sponge. However, while *circHipk2* acting as miR-124 sponge has been reported,[32] *Cdr1as* is not expressed in N2a cells. For these reasons, circTulp4 was selected for further functional analysis. A reduction in *circTulp4* levels leads to downregulation of miR-204-5p and miR-26a-5p targets, including *Meis2*, *Cdh2*, *Mitf*, and *Pde4b in vitro* (Figure 4F). *Cdh2* may be important for transcriptional control and regeneration of injured retinal ganglion cell axons.[33,34] *Mitf* controls development and function of the retinal pigment epithelium.[35] *Pde4b* is expressed in the inner segment, outer segment, and outer plexiform layer of rod photoreceptors, and it is an important regulator of signal transduction processes.[36] These genes were reported to be involved in retinal development and function. The significant phenotype of AAV-circTulp4-shRNA-treated retinas indicated an essential role for *circTulp4* in retinal development and function.

A key finding of our study was that circRNAs were found to be dysregulated at a much earlier time point than that of disease onset in the rd8 mouse model.[30] circRNA levels changed significantly compared to those of linear transcripts, whereas the structure and function of the retina in rd8 mice changed only slightly at P30 (Figures 6A and 6B). circRNAs seemed to be more sensitive and dynamic than linear transcripts in the rd8 model. Furthermore, the upregulation of *circTulp4* and *circHipk2* led to significant increases in the target genes of their sponged miRNAs (miR-204-5p, miR-26a-5p, and miR-124-3p) (Figure 6C), including genes involved in retinal development and function. These results further validated that *circTulp4* functions as a ceRNA *in vivo*. Our data also implied that certain and precise circRNA levels are required during the normal development of the retina. circRNAs are stable, have tissue- and development-specific expression, and can be found in plasma, cell-free saliva, and exosomes,[14,37,38] so we hypothesized that circRNAs might be a potential biomarker for retinal degenerative disease.

In summary, we generated a profile of the entire picture of circRNAs during retinal development and identified circRNA signatures in developing and degenerating retinas. Our findings provided a reference map and new insights into deciphering the biological roles of circRNAs in retinal development and degeneration.

MATERIALS AND METHODS

Cell Culture and Transfection

Human embryonic kidney (293D) cells and mouse neuroblastoma N2a cells were cultured at 37°C with 5% CO_2 in DMEM with 10% fetal bovine serum. Cells were transfected with the described plasmids using Lipofectamine 2000 (Life Technologies) according to the manufacturer's protocol.

Animals

C57BL/6J and rd8 mice obtained from Charles River (China) were bred in a 12-h light/12-h dark cycle, had free access to food and water, and were maintained in the animal facility of Wenzhou Medical University; the study obtained ethics approval (no. SYXK 2015-0009). The ages of the mice were indicated in the results, and only male mice were used in our study.

RNA Isolation and qRT-PCR

RNAs were extracted from the N2a cells and retinas by using the RNeasy kit (QIAGEN). Nuclear and cytoplasmic fractions were extracted (PARIS kit protein and RNA isolation system, Invitrogen). Complementary DNA (cDNA) was synthesized using a random primer (Promega) and quantified using FastStart Universal SYBR Green Master Mix (Roche). The divergent and convergent primers were designed for circRNAs and linear transcripts, respectively, and GAPDH was used as the reference gene (Table S2).

circRNA Sequencing Analysis

After retinas were dissected and mashed, RNAs were extracted with TRIzol reagent (Life Technologies) and an RNeasy mini kit (QIAGEN). Two samples were prepared from each developmental

stage, and each sample contained pooled retinas from multiple mice. RNA purity was detected using a NanoDrop spectrophotometer (Thermo Fisher Scientific), and the RNA concentration was measured with a Qubit RNA HS assay kit in a Qubit 3.0 fluorometer (Life Technologies). RNA integrity was assessed using an Agilent RNA 6000 Pico kit for the Agilent Bioanalyzer 2100 system (Agilent Technologies) (Table S4). After finishing the RNA quality test, 2 μg of total RNA was ribo-depleted using a KAPA RiboErase kit (Kapa Biosystems, USA). Sequencing libraries were generated by using the KAPA stranded RNA-seq kit (Kapa Biosystems, USA) according to the manufacturer's recommendations, and index codes were added to identify sequences. Libraries were pooled and sequenced on the Illumina X-Ten PE150 platform. The number of reads per sample is listed in Table S5. Raw data were submitted to the NCBI GEO database (GEO: GSE137128). Computational analysis was performed as described in a previous report.[1] FASTQ data were mapped to the mouse reference genome mm9. circRNA detection and quantification were performed using the find_circ and CIRI software,[26,39] and the circRNA abundance was measured through the total number of reads (head-to-tail junction). To examine circRNA relative expression (CLR), the following equation was used: CLR = no. of reads_circular/maximum (no. of reads_linear_5-prime, no. of reads_linear_3-prime).

circRNA Expression During Retinal Development

To summarize and compare circRNA expression, circRNAs were assigned to four classes: (1) "high," top 5% most highly expressed circRNAs; (2) "medium," between the 80th and 95th percentiles of circRNA expression; (3) "low," all other circRNAs; and (4) "not detected," circRNAs that were not detected in a particular sample.

Conservation Analysis between Humans and Mice

The conservation of circRNAs between humans and mice was analyzed. circRNA data in the human retina were derived from our published data.[23] We used a homologous splice site as a rationale, and the UCSC liftOver tool was used to convert the 5′ and 3′ flank coordinates of mouse circRNA to human genome coordinates.[24] Subsequently, circRNAs were classified into the following categories: (1) "not aligned" indicated that sites could not be mapped to the human genome; (2) "no homologous circRNA" indicated that no splice sites were detected within 2 nt of the converted genome coordinates; (3) "with homologous 5′ splice site" indicated that only the 5′ splice site was shared by the circRNAs in humans; (4) "with homologous 3′ splice" indicated that only the 3′ splice site was shared by the circRNAs in humans; (5) "with both splice sites" indicated that both the 3′ and 5′ splice sites were shared by the circRNAs in humans; and (6) "homologous circRNA" indicated that a circRNA spliced from sites within 2 nt of the splice sites predicted by liftOver was found in humans.

Bioinformatics Analysis

The binding patterns between miRNAs and circRNAs were predicted using Miranda (http://miranda.org.uk/),[40] RNAhybrid (https://omictools.com/rnahybrid-tool),[41] and TargetScan (http://www.targetscan.org/vert_72/).[42]

Luciferase Assay

The dual-luciferase reporter psi-CHECK2 plasmid was used in our study. The entire mouse *circAnkib1*, *circHipk2*, and *circTulp4* segments were amplified by PCR using mouse retinal cDNA as a template; the primers are listed in Table S6. The PCR products were inserted into the psi-CHECK2 plasmid to create Luci-circAnkib1, Luci-circHipk2, and Luci-circTulp4, which were cotransfected into 293D cells with a mimic-miRNA. A mimic-negative control (NC) and the psi-CHECK2 empty vector were used as negative controls. After transfection for 48 h, firefly and Renilla substrates were added in sequentially, and the corresponding luminescence was measured on a microplate spectrophotometer.

RNA Immunoprecipitation Assay

The retinas were isolated and collected in lysis buffer (Thermo Scientific) containing PMSF and propidium iodide (PI); then, proteins were extracted and quantified using a bicinchoninic acid (BCA) kit (Thermo Scientific). Three hundred micrograms of protein was incubated with 4 μg of Ago2 (Abcam) or immunoglobulin (Ig)G antibodies (Thermo Scientific) and incubated at 4°C overnight with shaking. Fifty microliters of protein A/G magnetic beads (Thermo Scientific) was added and incubated at 4°C for 2–4 h with shaking. The beads were separated using a magnetic strip and then washed four times with 0.2% Nonidet P-40 in PBS. The beads were suspended in TRIzol reagent, and RNA was extracted and subjected to qRT-PCR analysis.

In Situ Hybridization

For ISH, a BaseScope reagent kit-RED and a circTulp4 probe targeting the junction site were designed and supplied by Advanced Cell Diagnostics (ACD). Cryosections of mouse retinas were dried completely at room temperature (RT) and treated with hydrogen peroxide and protease plus; then, probe hybridization was performed strictly according to the manufacturer's protocol. Images were acquired using a microscope (Nikon Eclipse).

TUNEL Assay

Apoptosis of retinal cells was assessed using a TUNEL assay (Beyotime, China) according to the manufacturer's protocol.

AAV8-Mediated circTulp4 Knockdown

To generate the AAV8-mmu-circTulp4 shRNA, the target sequence 5′-ACAACAGTGAGAGTTGTAA-3′ was cloned into a GV478 vector containing U6-MCS-CAG-EGFP. The control sequence 5′-CG CTGAGTACTTCGAAATGTC-3′ was cloned into a GV478 vector to serve as the control. The AAV8-mmu-circTulp4-shRNA and AAV-EGFP control titers were 1.27×10^{13} and 1.50×10^{13} transduction units (TU)/mL, respectively. The subretinal injection of AAV was performed as previously described.[43] C57BL/6J mice at P30 were anesthetized with a mixture of ketamine and xylazine. A small incision was created in the lens near the sclera with a sharp 30-gauge

needle. Then, 1 μL (1.27×10^{13} TU/mL) of AAV8-mmu-circTulp4-shRNA and an equal dose of control vector AAV-EGFP were injected slowly into the subretinal space of the right eye and left eye, respectively, using a blunt 5-μL Hamilton syringe held in a micromanipulator. All injections were performed bilaterally.

Focal ERG

The focal ERG was carried out as described in the instrument manuals (Phoenix Research Laboratories) and as previously described.[37] Briefly, mice were dark-adapted overnight and anesthetized as described previously. Before light stimulation, their pupils were dilated, and their corneas were anesthetized with 0.5% phenylephrine and 0.5% tropicamide. A drop of 1% methyl cellulose was applied on the cornea to improve conjunction with a corneal gold wire electrode. Ground electrodes and a referential needle were punctured into the tail and cheek, respectively. The "Aming light" was turned to a high value to ensure the biggest light spot around the optic nerve head; the size of the stimulus region was approximately two-thirds of the entire retina. Scotopic ERG was performed five times with an inter-stimulus interval of 20 s at a 3.0 log cd·s/m^2 stimulus intensity. After 10 min of light adaptation with a background illumination of 5.3 cd/m^2, the mice were subjected to photopic measurements obtained five times at 3.3 log cd·s/m^2 with a 20-s inter-stimulus. The a-wave and b-wave amplitudes of the scotopic and photopic responses from mice treated with AAV-circTulp4 shRNA and AAV-EGFP were recorded and averaged.

Fundus Photography

Mice injected with AAV-circTulp4 shRNA and AAV-EGFP were anesthetized as described previously. Before the examination, 2.5% hydroxypropyl methylcellulose was dropped into the eyes to improve the connection with the machine (Micron IV, Phoenix Research Labs), and then fundus photography was performed.

SUPPLEMENTAL INFORMATION

Supplemental Information can be found online at https://doi.org/10.1016/j.omtn.2019.11.016.

AUTHOR CONTRIBUTIONS

X.-J.C., X.-Y.W., H.-Q.Z, C.-J. Z., K.-C.W., M.-L.L., Y.-Y.J., Y.M., L.X., and L.-F.S. performed the research; H.-Q.Z and M.Z. analyzed the data; Z.-B.J. and X.-J.C designed the research; Z.-B.J. and X.-J.C wrote the paper.

CONFLICTS OF INTEREST

The authors declare no competing interests.

ACKNOWLEDGMENTS

This study was supported by the National Natural Science Foundation of China (81870690 and 81970838); National Key R&D Program of China (2017YFA0105300 and 2017YFB0403700); Zhejiang Provincial Natural Science Foundation of China (LD18H120001); Zhejiang Provincial Key Research and Development Program (2015C03029); and the 111 Project (D16011).

REFERENCES

1. Rybak-Wolf, A., Stottmeister, C., Glažar, P., Jens, M., Pino, N., Giusti, S., Hanan, M., Behm, M., Bartok, O., Ashwal-Fluss, R., et al. (2015). Circular RNAs in the mammalian brain are highly abundant, conserved, and dynamically expressed. Mol. Cell *58*, 870–885.
2. Han, J., Gao, L., Dong, J., Bai, J., Zhang, M., and Zheng, J. (2017). The expression profile of developmental stage-dependent circular RNA in the immature rat retina. Mol. Vis. *23*, 457–469.
3. Glažar, P., Papavasileiou, P., and Rajewsky, N. (2014). circBase: a database for circular RNAs. RNA *20*, 1666–1670.
4. Guo, J.U., Agarwal, V., Guo, H., and Bartel, D.P. (2014). Expanded identification and characterization of mammalian circular RNAs. Genome Biol. *15*, 409.
5. Salzman, J., Chen, R.E., Olsen, M.N., Wang, P.L., and Brown, P.O. (2013). Cell-type specific features of circular RNA expression. PLoS Genet. *9*, e1003777.
6. Lu, C., Sun, X., Li, N., Wang, W., Kuang, D., Tong, P., Han, Y., and Dai, J. (2018). circRNAs in the tree shrew (*Tupaia belangeri*) brain during postnatal development and aging. Aging (Albany N.Y.) *10*, 833–852.
7. Chen, B.J., Yang, B., and Janitz, M. (2018). Region-specific expression of circular RNAs in the mouse brain. Neurosci. Lett. *666*, 44–47.
8. Westholm, J.O., Miura, P., Olson, S., Shenker, S., Joseph, B., Sanfilippo, P., Celniker, S.E., Graveley, B.R., and Lai, E.C. (2014). Genome-wide analysis of drosophila circular RNAs reveals their structural and sequence properties and age-dependent neural accumulation. Cell Rep. *9*, 1966–1980.
9. Hansen, T.B., Jensen, T.I., Clausen, B.H., Bramsen, J.B., Finsen, B., Damgaard, C.K., and Kjems, J. (2013). Natural RNA circles function as efficient microRNA sponges. Nature *495*, 384–388.
10. You, X., Vlatkovic, I., Babic, A., Will, T., Epstein, I., Tushev, G., Akbalik, G., Wang, M., Glock, C., Quedenau, C., et al. (2015). Neural circular RNAs are derived from synaptic genes and regulated by development and plasticity. Nat. Neurosci. *18*, 603–610.
11. Kleaveland, B., Shi, C.Y., Stefano, J., and Bartel, D.P. (2018). A network of noncoding regulatory RNAs acts in the mammalian brain. Cell *174*, 350–362.e17.
12. Piwecka, M., Glažar, P., Hernandez-Miranda, L.R., Memczak, S., Wolf, S.A., Rybak-Wolf, A., Filipchyk, A., Klironomos, F., Cerda Jara, C.A., Fenske, P., et al. (2017). Loss of a mammalian circular RNA locus causes miRNA deregulation and affects brain function. Science *357*, eaam8526.
13. Zhao, Z.J., and Shen, J. (2017). Circular RNA participates in the carcinogenesis and the malignant behavior of cancer. RNA Biol. *14*, 514–521.
14. Li, Y., Zheng, Q., Bao, C., Li, S., Guo, W., Zhao, J., Chen, D., Gu, J., He, X., and Huang, S. (2015). Circular RNA is enriched and stable in exosomes: a promising biomarker for cancer diagnosis. Cell Res. *25*, 981–984.
15. Peng, L., Yuan, X.Q., and Li, G.C. (2015). The emerging landscape of circular RNA ciRS-7 in cancer (Review). Oncol. Rep. *33*, 2669–2674.
16. Lukiw, W.J. (2013). Circular RNA (circRNA) in Alzheimer's disease (AD). Front. Genet. *4*, 307.
17. Ghosal, S., Das, S., Sen, R., Basak, P., and Chakrabarti, J. (2013). Circ2Traits: a comprehensive database for circular RNA potentially associated with disease and traits. Front. Genet. *4*, 283.
18. Shan, K., Liu, C., Liu, B.H., Chen, X., Dong, R., Liu, X., Zhang, Y.Y., Liu, B., Zhang, S.J., Wang, J.J., et al. (2017). Circular noncoding RNA HIPK3 mediates retinal vascular dysfunction in diabetes mellitus. Circulation *136*, 1629–1642.
19. Zhang, S.J., Chen, X., Li, C.P., Li, X.M., Liu, C., Liu, B.H., Shan, K., Jiang, Q., Zhao, C., and Yan, B. (2017). Identification and characterization of circular RNAs as a new class of putative biomarkers in diabetes retinopathy. Invest. Ophthalmol. Vis. Sci. *58*, 6500–6509.
20. Chen, Y., Li, C., Tan, C., and Liu, X. (2016). Circular RNAs: a new frontier in the study of human diseases. J. Med. Genet. *53*, 359–365.
21. Zhang, Z., Yang, T., and Xiao, J. (2018). Circular RNAs: promising biomarkers for human diseases. EBioMedicine *34*, 267–274.
22. Daum, J.M., Keles, Ö., Holwerda, S.J., Kohler, H., Rijli, F.M., Stadler, M., and Roska, B. (2017). The formation of the light-sensing compartment of cone photoreceptors coincides with a transcriptional switch. eLife *6*, e31437.

23. Sun, L.F., Zhang, B., Chen, X.J., Wang, X.Y., Zhang, B.W., Ji, Y.Y., Wu, K.C., Wu, J., and Jin, Z.B. (2019). Circular RNAs in human and vertebrate neural retinas. RNA Biol. *16*, 821–829.

24. Gao, Y., Zhang, J., and Zhao, F. (2018). Circular RNA identification based on multiple seed matching. Brief. Bioinform. *19*, 803–810.

25. Hinrichs, A.S., Karolchik, D., Baertsch, R., Barber, G.P., Bejerano, G., Clawson, H., Diekhans, M., Furey, T.S., Harte, R.A., Hsu, F., et al. (2006). The UCSC Genome Browser database: update 2006. Nucleic Acids Res. *34*, D590–D598.

26. Li, X., Yang, L., and Chen, L.L. (2018). The biogenesis, functions, and challenges of circular RNAs. Mol. Cell *71*, 428–442.

27. Cocquerelle, C., Daubersies, P., Majérus, M.A., Kerckaert, J.P., and Bailleul, B. (1992). Splicing with inverted order of exons occurs proximal to large introns. EMBO J. *11*, 1095–1098.

28. Nigro, J.M., Cho, K.R., Fearon, E.R., Kern, S.E., Ruppert, J.M., Oliner, J.D., Kinzler, K.W., and Vogelstein, B. (1991). Scrambled exons. Cell *64*, 607–613.

29. Winter, J., Jung, S., Keller, S., Gregory, R.I., and Diederichs, S. (2009). Many roads to maturity: microRNA biogenesis pathways and their regulation. Nat. Cell Biol. *11*, 228–234.

30. Chang, B., Hawes, N.L., Nishina, P.M., Smith, R.S., Davisson, M.T., and Heckenlively, J.R. (1999). Two new mouse models of retinal degeneration (rd8 and Rd9). Invest. Ophthalmol. Vis. Sci. *40* (*Suppl*), S976.

31. Memczak, S., Jens, M., Elefsinioti, A., Torti, F., Krueger, J., Rybak, A., Maier, L., Mackowiak, S.D., Gregersen, L.H., Munschauer, M., et al. (2013). Circular RNAs are a large class of animal RNAs with regulatory potency. Nature *495*, 333–338.

32. Huang, R., Zhang, Y., Han, B., Bai, Y., Zhou, R., Gan, G., Chao, J., Hu, G., and Yao, H. (2017). Circular RNA *HIPK2* regulates astrocyte activation via cooperation of autophagy and ER stress by targeting *MIR124-2HG*. Autophagy *13*, 1722–1741.

33. Liu, Q., Londraville, R.L., Azodi, E., Babb, S.G., Chiappini-Williamson, C., Marrs, J.A., and Raymond, P.A. (2002). Up-regulation of cadherin-2 and cadherin-4 in regenerating visual structures of adult zebrafish. Exp. Neurol. *177*, 396–406.

34. Li, B., Paradies, N.E., and Brackenbury, R.W. (1997). Isolation and characterization of the promoter region of the chicken N-cadherin gene. Gene *191*, 7–13.

35. Saule, S. (2012). Both PAX6 and MITF are required for pigment epithelium development in vivo. Pigment Cell Melanoma Res. *25*, 541–543.

36. Whitaker, C.M., and Cooper, N.G.F. (2009). The novel distribution of phosphodiesterase-4 subtypes within the rat retina. Neuroscience *163*, 1277–1291.

37. Bahn, J.H., Zhang, Q., Li, F., Chan, T.M., Lin, X., Kim, Y., Wong, D.T., and Xiao, X. (2015). The landscape of microRNA, Piwi-interacting RNA, and circular RNA in human saliva. Clin. Chem. *61*, 221–230.

38. Vo, J.N., Cieslik, M., Zhang, Y., Shukla, S., Xiao, L., Zhang, Y., Wu, Y.M., Dhanasekaran, S.M., Engelke, C.G., Cao, X., et al. (2019). The candscape of circular RNA in cancer. Cell *176*, 869–881.e13.

39. Gao, Y., Wang, J., and Zhao, F. (2015). CIRI: an efficient and unbiased algorithm for de novo circular RNA identification. Genome Biol. *16*, 4.

40. Turner, D. (1986). An overview of Miranda. SIGPLAN Not. *21*, 158–166.

41. Krüger, J., and Rehmsmeier, M. (2006). RNAhybrid: microRNA target prediction easy, fast and flexible. Nucleic Acids Res. *34*, W451-4.

42. Lewis, B.P., Burge, C.B., and Bartel, D.P. (2005). Conserved seed pairing, often flanked by adenosines, indicates that thousands of human genes are microRNA targets. Cell *120*, 15–20.

43. Xiang, L., Chen, X.J., Wu, K.C., Zhang, C.J., Zhou, G.H., Lv, J.N., Sun, L.F., Cheng, F.F., Cai, X.B., and Jin, Z.B. (2017). miR-183/96 plays a pivotal regulatory role in mouse photoreceptor maturation and maintenance. Proc. Natl. Acad. Sci. USA *114*, 6376–6381.

OMTN, Volume *19*

Supplemental Information

The Circular RNome of Developmental Retina in Mice

Xue-Jiao Chen, Zi-Cheng Zhang, Xiao-Yun Wang, Heng-Qiang Zhao, Meng-Lan Li, Yue Ma, Yang-Yang Ji, Chang-Jun Zhang, Kun-Chao Wu, Lue Xiang, Lan-Fang Sun, Meng Zhou, and Zi-Bing Jin

Supplementary Figure 1. circRNA expression analysis at E18.5 vs. P1, P1 vs. P7, P7 vs. P14, P14 vs. P30.

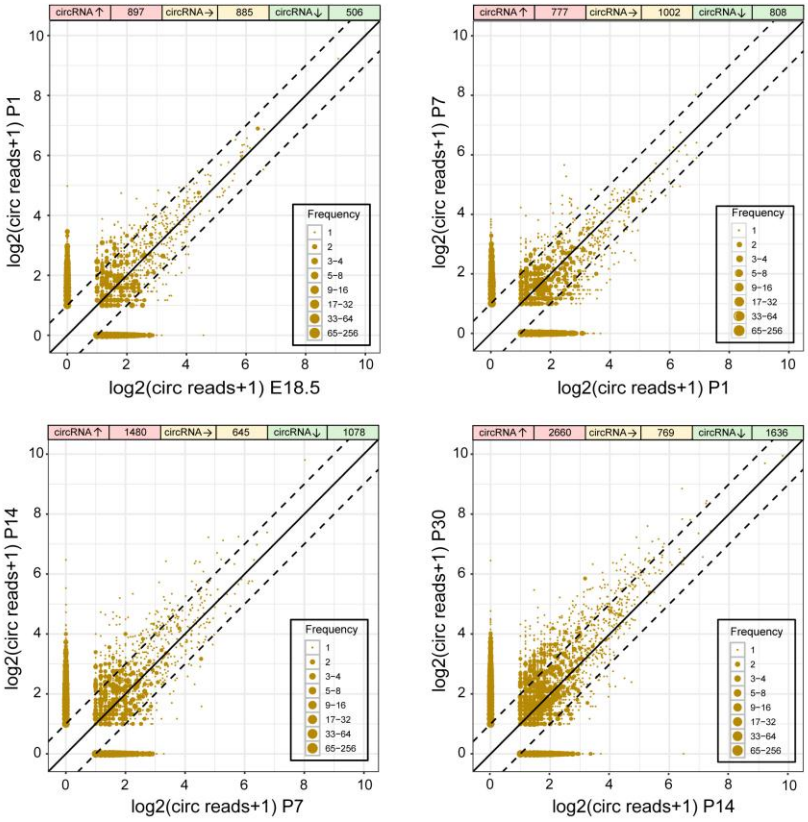

Supplementary Figure 2. Head to tail junction sequences of circRNAs.

mmu_circ_0001878|Cdr1as

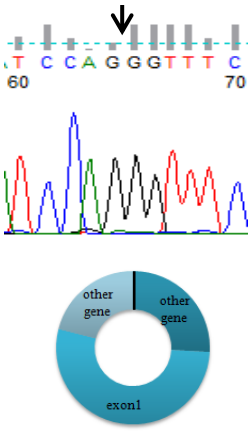

mmu_circ_0001757|Bbs9

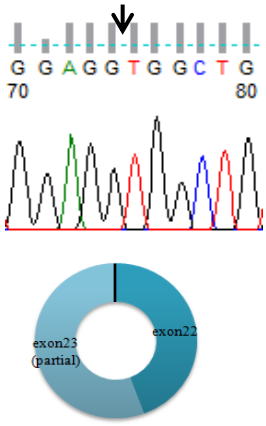

mmu_circ_0001468|Hipk2

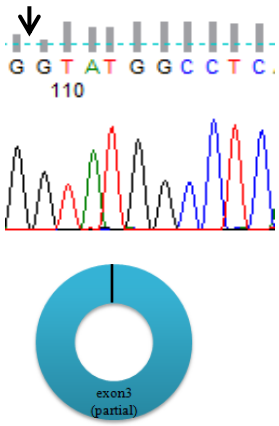

mmu_circ_0001692|Arhgap10

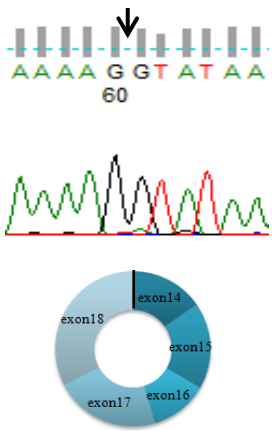

mmu_circ_0000377|Arhgap5

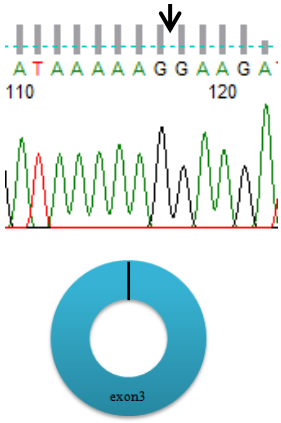

mmu_circ_0001311|Ankib1

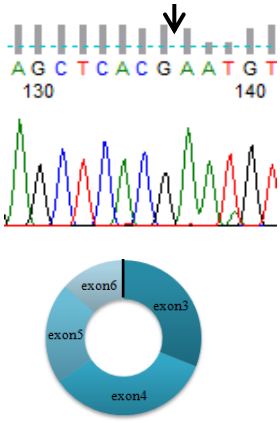

mmu_circ_0000723|Tulp4

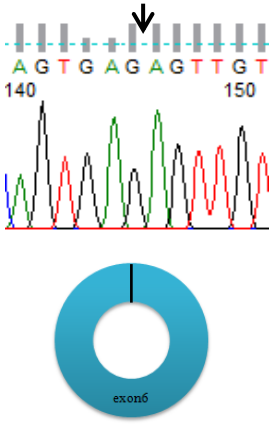

mmu_circ_0001624|Mettl9

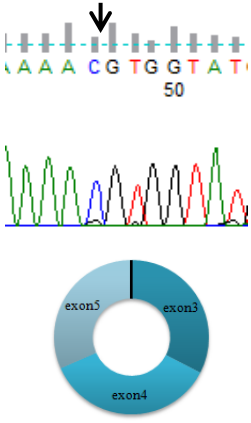

Supplementary Figure 3. Comparsion the results between RNA-seq and qRT-PCR.

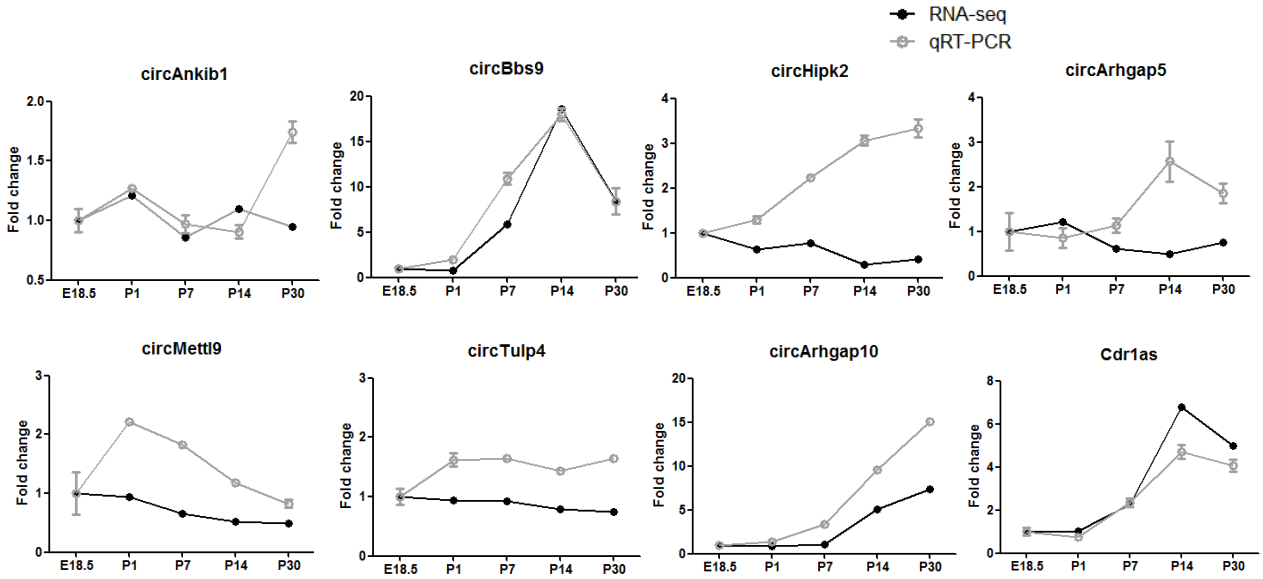

Supplementary Figure 4. (A) circRNA expression change between P7 and P1 are positively correlated with host genes expression changes. (B) Summary of expression changes between circRNA and host gene at P7 vs. P1. (C) circRNA expression change between P14 and P1 are positively correlated with host genes expression changes. (D) Summary of expression changes between circRNA and host gene at P14 vs. P1.

A

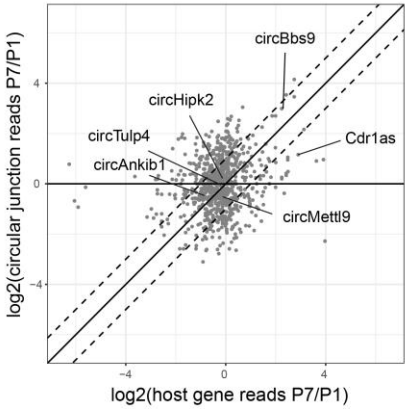

C

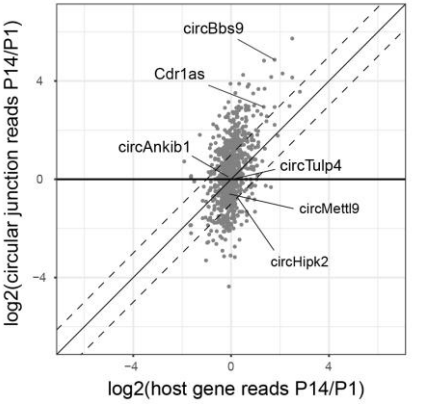

B

P7 vs. P1

	mRNA ↑	mRNA →	mRNA ↓
circRNA ↑	235	733	61
circRNA →	67	414	37
circRNA ↓	113	705	153

D

P14 vs. P1

	mRNA ↑	mRNA →	mRNA ↓
circRNA ↑	115	833	17
circRNA →	7	451	8
circRNA ↓	22	1442	295

Supplementary Figure 5. luciferase assay detection the binding between miRNAs and circAnkib1 (A), circBbs9 (B)and circMettl9 (C) in 293D cell.

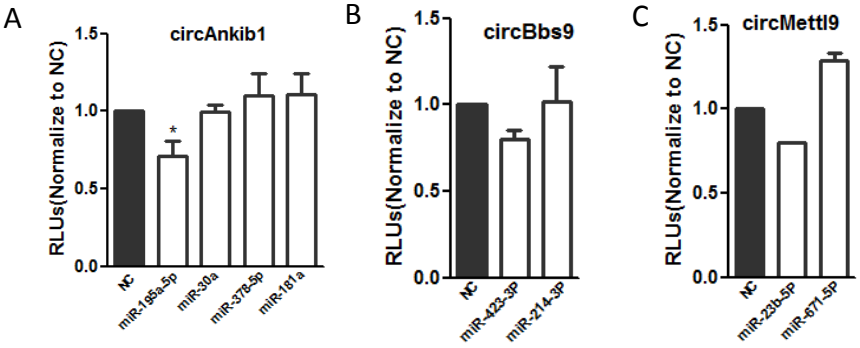

Supplementary Figure 6. The target sites of miRNAs in corresponding circRNAs

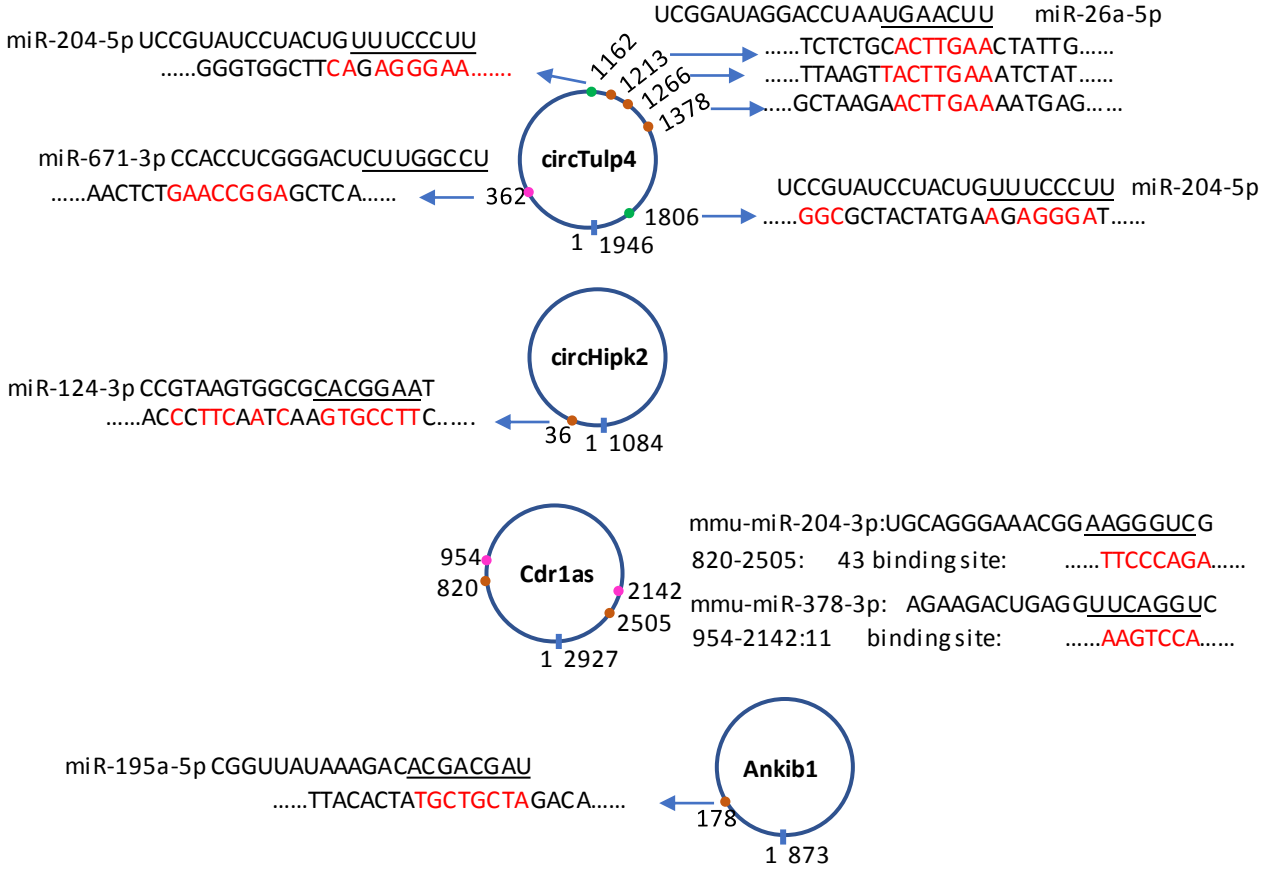

Supplementary Figure 7. qRT-PCR identify the interference efficiency of si-circTulp4 in N2a cell.

A

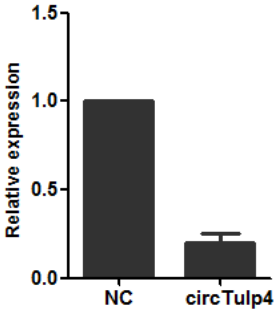

Supplementary Figure 8. Representative ERG response recording of retina after AAV-circTulp4 shRNA and AAV-EGFP subretinal injection. Representative ERG curve that consisted of a negative a-wave and a positive b-wave; the distance between dashed lines labeled by a or b is the amplitude of the a and b wave, respectively.

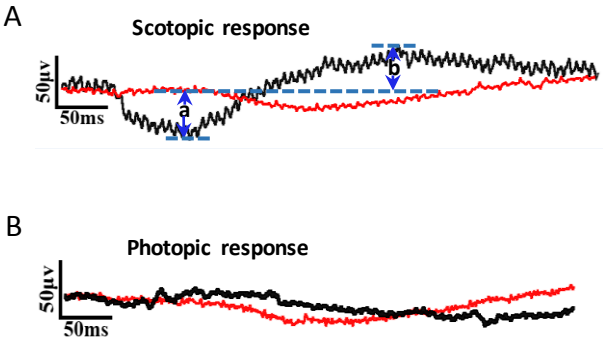

Supplementary Figure 9. qRT-PCR detection of miR-204-5p, miR-26a-5p (a), miR-204-5p and miR-26a-5p target genes (b) and target s of Meis2 (C) in mouse retina after AAV-circTulp4 shRNA and AAV-EGFP subretinal injection.

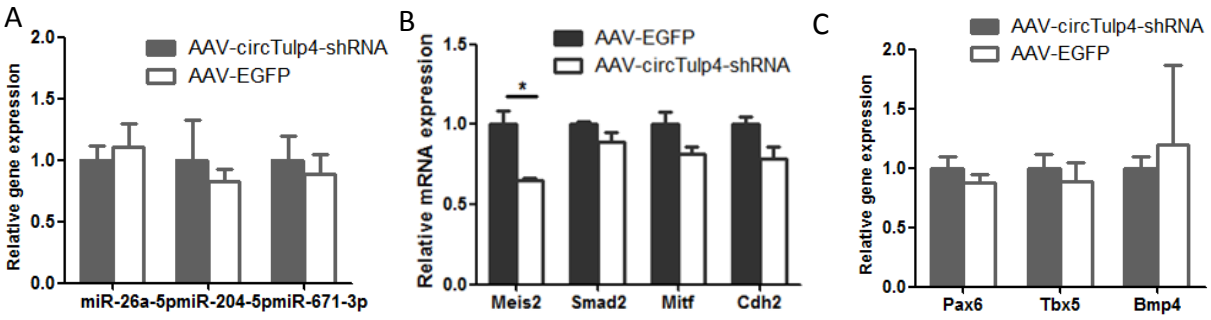

Supplementary Figure 10. Negative control DAPB of ISH in mouse retina.

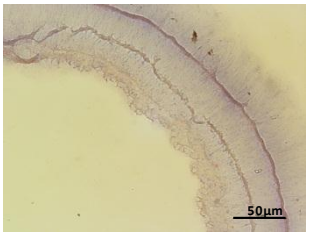

20X

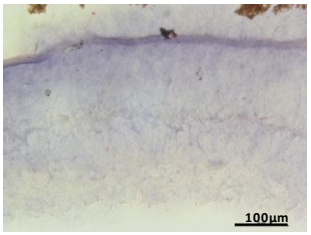

40X

Supplementary Table 1. The replicates overlap of circRNAs across the five stages.

	E18.5	P1	P7	P14	P30
E18.5	301	736	647	705	802
P1	736	452	813	862	983
P7	647	813	384	929	1078
P14	705	862	929	697	1543
P30	802	983	1078	1543	2147

Supplementary Table 2. Primers used in QPCR.

	Forward	Reverse
mmu_circ_0001624	GGTCATCCTGGCATTGGT	GCCAGCCAGATTTCTCAATG
mmu_circ_0001468	TATCCATGCTGACCTCAAACC	CACACTACAGAAGGCACTTGA
mmu_circ_0000723	CCCAAGAGTGAGAAGGAGAAAC	CGGTTAATTCAGGAGCCATCA
mmu_circ_0001311	CCGAAGAAATAGAAGCGGAGTAT	GATGAGTGCTTTGCGGAATTT
mmu_circ_0001757	TGGAGTAATGCTAATGAGTTGAGG	GCTGAGACTTCAGGCATGG
mmu_circ_0000629	GGGTCCATGAGGGTTGTATT	CGAGGGCTGAACTCTTCTATG
mmu_circ_0000377	AGACATCGTGGAAGTGAAGAAG	GGGTCGAGGCTCTTTGTTT
mmu_circ_0001878	CGCAGTGTCTCCAGTGTATC	TGCAGTTGCTGGAAGACC
lin-Mettl9	GAAAACGTAGGTGGCAAGTGG	AGCTTCGACGACAAAGCCGGC
lin-Bbs9	ACCTGCAGTGCTCGTATC	GGGTACCTTGCAACTTTACATC
lin-Tulp4	TCGTCTCTGTTCCTACCTCTC	CAAAGTCTCGCATGTTGTTGG
lin-Ankib1	AGCACTTTCGATCTCCCAGAG	TGCAGAGCGACTGGCAGGGCT
lin-Arhgap5	TGACAGCAGACAACTTATCCATC	CCACAGTGTTCGCAGTTTCTA
lin-Hipk2	GGTCATTGACTTTGGTTC	CTTCACACTACAGAAGGC
Q-m-Mitf	CCTCTGAAGAGCAGCAGTTCT	CTCCCTGCGCTCCTGCTCCTG
Q-m-Meis2	GCAATCTATGGGCACCCGTTG	GGAACAGACGTCTCCGCCGGC
Q-m-Stat3	CAGTTTCTGCAGAGCAGGTAT	CTGGGCTGCCGTGGCTGCCGT
Q-m-Smad2	ACCATACCAAGGTCTCTTGAT	ATGATGACTGTGAAGGTCCGG
Q-m-Ulk2	GGTTCTCCAAGATCTGCAGTA	TCTTCGTCCTCCTGTCTGCAC
Q-m-Rd3	GCCATCCTCAGGTTCAGGCAG	GGTTCGGATGTCACTGGCAAA
Q-m-Pde4d	CGGAGCAAAAGTGCCTCTGAG	ACTTGAGTCTGCAGATGTGAC
Q-m-Bbs9	GGGAACGGCCACGATAAAATC	ATCTTCAGCCTGAGGCCCACC
Q-m-Rnf217	AGCTCTCAGGTACAACTTGGC	CTTGATAGAGTCCTCATGGGT
Q-m-Slc6a6	AATGGTGGAGGTGCGTTCCTC	ACAGATCTTCTCCCAGCAGGT
Q-m-GAPDH	AGGTCGGTGTGAACGGATTTG	TGTAGACCATGTAGTTGAGGTCA

Supplementary Table 3. siRNA target sequence.

	sequence
si-circTulp4	ACAACAGTGAGAGTTGTAA
si-nc	CGCTGAGTACTTCGAAATGTC

Supplementary Table 4. The concentration and quality of RNA used for RNA-seq. RNAs were extracted with the TRIzol reagent and RNeasy mini kit (Qiagen).

Sample	Concentration (ng/g)	OD (260/280)	Quality (RIN)	Sample	Concentration (ng/g)	OD (260/280)	Quality (RIN)
E18.5-1	21.3	1.94	9.7	P7-2	3.6	1.94	10
E18.5-3	3.39	1.97	10	P14-1	4.48	1.88	9
P1-1	5.22	1.93	10	P14-3	3.41	1.97	8.4
P1-2	5.84	1.95	10	P30-2	3.3	1.87	8.6
P7-1	4.17	1.88	9.6	P30-3	3	1.91	8.7

Supplementary Table 5. Filtration and quality control of raw data. Raw reads/bases: reads/bases from original sequence, clean reads/bases: reads/bases from filtrated sequence, clean Q30: ratio of clean bases with quality score > 30 in total base.

Sample ID	raw reads	Clean reads	raw bases (Mb)	Clean bases (Mb)	clean Q30
E18-5-1	75997539	75243933	22798	20775	97.24%
E18-5-3	77546099	76967520	23262	21379	97.23%
P1-1	77543283	76978763	23262	21384	97.45%
P1-2	70357032	69759219	21106	19432	97.41%
P14-1	68346318	67787248	20502	18721	97.22%
P14-3	75127421	74552395	22538	20711	97.41%
P30-2	77687557	77030376	23306	21548	97.37%
P30-3	78367493	77531361	23510	21464	97.06%
P7-1	80589244	79991846	24176	22100	97.44%
P7-2	65589116	65124438	19676	18050	97.43%

Supplementary Table 6. Primers for luciferase assay.

	Forward	Reverse
Lucif-m-circ_0001878	CTCGAGGGTTTCCAGTGGTGCCAGTAC	GCGGCCGCCCAGAAAACCTGAATGTC
Lucif-m-circ_0001468	CTCGAGGTATGGCCTCACATGTGC	GCGGCCGCCGGTAGTATCTGGATTGC
Lucif-m-circ_0000723	GCGGCCGCAGTTGTAAGAGTCCATCCAGG	GTTTAAACCTCACTGTTGTGGCCTCGCAG
Lucif-m-circ_0001311	CTCGAGAATGTGAAACATGTTGTA	GCGGCCGCCGTGAGCTCGAAGCAGTG
Lucif-m-circ_0001757	CTCGAGGTGGCTGTACTCCAATCCCAG	GCGGCCGCCTCCAGAGATGAGCTTGG
Lucif-m-circ_0001624	CTCGAGTGGTATGTGTGCAACAGAGAG	GCGGCCGCCGTTTTCTACATAGGGAT